Original Article

Feasibility of chest spiral 3D ultrashort echo time magnetic resonance imaging for intrathoracic metastasis work-up in breast cancer

Kyung Jin Nam[1]^, Taewoo Kang[2]^, Ji Won Lee[3]^, Minhee Hwang[3]^, Jin You Kim[3]^, Jeong A Yeom[1]^, Yeon Joo Jeong[1]^

[1]Department of Radiology, Research Institute for Convergence of Biomedical Science and Technology, Pusan National University Yangsan Hospital, Pusan National University School of Medicine, Yangsan, Korea; [2]Busan Cancer Center, Pusan National University Hospital, Department of Surgery, Pusan National University School of Medicine and Biomedical Research Institute, Busan, Korea; [3]Department of Radiology, Pusan National University Hospital, Pusan National University School of Medicine and Biomedical Research Institute, Busan, Korea

Contributions: (I) Conception and design: KJ Nam, JW Lee, YJ Jeong; (II) Administrative support: None; (III) Provision of study materials or patients: T Kang; (IV) Collection and assembly of data: KJ Nam, JW Lee, YJ Jeong; (V) Data analysis and interpretation: KJ Nam, JW Lee, YJ Jeong; (VI) Manuscript writing: All authors; (VII) Final approval of manuscript: All authors.

Correspondence to: Yeon Joo Jeong, MD, PhD. Department of Radiology, Research Institute for Convergence of Biomedical Science and Technology, Pusan National University Yangsan Hospital, Pusan National University School of Medicine, 20, Geumo-ro, Mulgeum-eup, Yangsan-si, Gyeongnam 50612, Korea. Email: jeongyj@pusan.ac.kr.

Background: Chest computed tomography (CT) is routinely performed to evaluate intrathoracic metastasis in patients with breast cancer, but radiation exposure and its potential carcinogenic risks are major drawbacks. Furthermore, pulmonary imaging by magnetic resonance imaging (MRI) is limited by low proton density, rapid signal decay, and sensitivity to respiratory and cardiac motions in lung tissue. Recently, a respiratory gating spiral three-dimensional (3D) ultrashort echo time (UTE) volume interpolated breath-hold examination (VIBE) sequence for lung MRI provides high spatial-resolution images with reasonable scan times. Our objective was to investigate the feasibility of chest spiral 3D UTE VIBE MRI to detect intrathoracic metastasis in breast cancer patients.

Methods: This retrospective study of a prospectively collected database was conducted between February and July 2019 after institutional review board approval. All participants provided informed consent for MRI scans. Ninety-three female patients with breast cancer were retrospectively enrolled and underwent preoperative breast MRI, including a chest spiral 3D UTE VIBE sequence. Two chest radiologists evaluated image qualities of intrapulmonary vessels and bronchial wall visibilities, the presence of pulmonary nodules, significant lymph nodes (LNs), and other lung abnormalities on spiral 3D UTE magnetic resonance (MR) images and compared them using chest CT as a reference standard.

Results: Intrapulmonary vessels and bronchial walls were visible up to sub-subsegmental and sub-subsegmental levels, respectively, on spiral 3D UTE MR images, and better than fair quality was obtained for artifact/noise and overall image quality for 95.7% and 98.9% of the patients, respectively. The overall detection rate for pulmonary nodules was 62.8% (59/94). Furthermore, 59 of the 81 solid nodules detected by CT were detected by spiral 3D UTE MRI (72.8%), and 31 of the 33 solid nodules (≥5 mm in diameter) detected by CT were identified by spiral 3D UTE MRI (93.9%). Significant LNs in the axillary area were similarly detected by spiral 3D UTE MRI and chest CT.

Conclusions: Preoperative breast MRI with a chest spiral 3D UTE sequence could be used to evaluate

^ ORCID: Kyung Jin Nam, 0000-0001-5118-1903; Taewoo Kang, 0000-0002-6279-0904; Ji Won Lee, 0000-0003-1800-8548; Minhee Hwang, 0000-0003-2603-616X; Jin You Kim, 0000-0002-9631-501X; Jeong A Yeom, 0000-0002-0328-7989; Yeon Joo Jeong, 0000-0002-1741-9604.

breast cancer and axillary LNs and intrathoracic metastasis simultaneously and offers a potential alternative to chest CT for breast cancer patients without additional radiation exposure.

Keywords: Ultrashort echo time (UTE); magnetic resonance imaging (MRI); stack-of-spirals acquisition; intrathoracic metastasis; breast cancer

Submitted Jun 27, 2023. Accepted for publication Sep 08, 2023. Published online Sep 25, 2023.
doi: 10.21037/jtd-23-1006
View this article at: https://dx.doi.org/10.21037/jtd-23-1006

Introduction

Chest computed tomography (CT) is routinely performed to evaluate intrathoracic metastasis in patients with breast cancer. However, CT examinations require ionizing radiation and pose carcinogenic risks (1). In addition, repeat CT conducted to follow up small nodules incidentally found by chest CT results in cumulative radiation exposure (1). On the other hand, pulmonary imaging by magnetic resonance imaging (MRI) is limited by low proton density, rapid signal decay, and sensitivity to respiratory and cardiac motions in lung tissues (1). A short echo time (TE) is essential for lung MRI sequences because of the short T2 and T2* values of lung tissues (2,3).

The recent development of the ultrashort echo time (UTE) MRI sequence enables lung MRI to be used in clinical practice (4-13), but lung MRI is disadvantaged by a long scan time due to inefficient k-space coverage (4,6,14). To overcome this limitation, we applied three-dimensional (3D) stack-of-spirals (spiral) acquisition to improve readout efficiency (15-17). Several studies have recently demonstrated that spiral 3D UTE sequences enable high-resolution morphological imaging of lungs and pulmonary nodule detection with high sensitivity (1,18,19). The purpose of this study was to investigate the feasibility of chest spiral 3D UTE volume interpolated breath-hold examination (VIBE) MRI to detect intrathoracic metastasis in breast cancer patients. We present this article in accordance with the STROBE reporting checklist (available at https://jtd.amegroups.com/article/view/10.21037/jtd-23-1006/rc).

Highlight box

Key findings

- Chest spiral three-dimensional (3D) ultrashort echo time (UTE) volume interpolated breath-hold examination magnetic resonance imaging (MRI) detected pulmonary nodules in breast cancer patients with a 62.8% overall nodule detection rate and a 93.9% solid nodule (≥5 mm) detection rate, which was clinically significant and produced images of acceptable quality.

What is known and what is new?

- A respiratory gating spiral 3D UTE sequence enables lung MRI to be used in clinical practice and provides high spatial-resolution images with reasonable scan times.
- A chest spiral 3D UTE sequence could be useful for evaluating pulmonary metastasis and significant lymph nodes in axillary area in patients with breast cancer.

What is the implication, and what should change now?

- Preoperative breast MRI, including a chest spiral 3D UTE sequence, could be used to evaluate breast cancer, axillary lymph nodes, and intrathoracic metastasis simultaneously without radiation exposure.

Methods

Study design and subjects

This retrospective study was conducted using a prospectively collected database to investigate the feasibility of utilizing chest spiral 3D UTE VIBE MRI to detect intrathoracic metastasis in breast cancer patients that registered consecutively for preoperative staging work-up at Pusan National University Hospital between February and July 2019. The study was conducted in accordance with the Declaration of Helsinki (as revised in 2013). The study protocol was approved by the institutional review board of Pusan National University Hospital (IRB No. 2306-001-127), and informed consent was obtained from all individual participants. The modified breast MRI protocol used included a spiral 3D UTE VIBE sequence of the chest to evaluate intrathoracic metastasis during preoperative work-up. One hundred and fourteen female breast cancer patients underwent preoperative modified breast MRI. The exclusion criteria were as follows: the patient who did not undergo chest CT (n=20) and an interval of >30 days

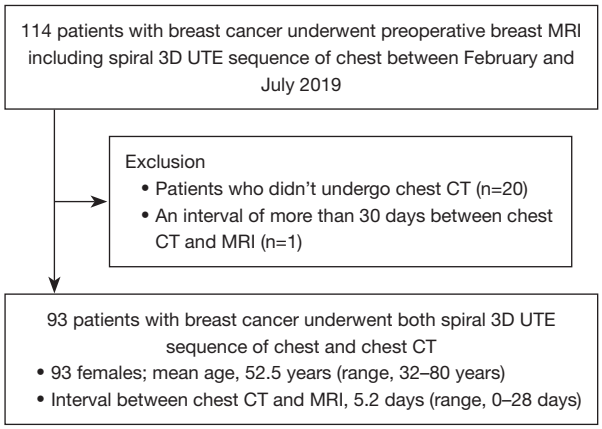

Figure 1 Flow chart of patient selection. MRI, magnetic resonance imaging; 3D, three-dimensional; UTE, ultrashort echo time; CT, computed tomography.

between chest CT and MRI (n=1). Eventually, 93 female patients were included in this study (*Figure 1*).

Magnetic resonance (MR) data acquisition

All patients underwent a respiratory-gated chest spiral 3D UTE VIBE sequence in the prone position during routine breast MRI using a 3-T MRI system (MAGNETOM Skyra, Siemens Healthcare, Erlangen, Germany). This sequence was obtained at a delay of 15 minutes after injecting a bolus gadobutrol (0.1 mmol/kg, Gadovist; Bayer Schering Pharma, Berlin, Germany) at a rate of 2 mL/s and a subsequent 20-mL saline flush. The parameters used were as follows: repetition time (TR) 3.4 ms/TE 0.1 ms, flip angle 5° degree, voxel size 1×1×1 mm^3, reconstruction matrix 320×320, and a field of view (FOV) of 400 mm × 400 mm in the coronal plane. Coronal UTE images were further reformatted as axial images by multiplanar reformatting.

Chest CT data acquisition

All CT images were obtained using a 256-row multi-detector CT scanner (Revolution CT, GE Medical Systems, Milwaukee, WI, USA) with contrast medium [100 mL of contrast medium (Xenetix 300; Guerbet); injection rate 2 mL/s], and images were obtained from the lung apex to the diaphragm, as was performed for MRI coverage. The following imaging parameters were applied: slice thickness =2.5 mm, collimation =64×0.6 mm, voltage =120 kVp, tube current setting =50 mA, FOV =329×329, and reconstruction interval =1.25 mm at a helical pitch of 1. The acquisition was performed during breath holding at the end of full inspiration. Lung and mediastinal windows were set at level −500, width 1,300, and level 40, width 400, respectively.

Image analysis

Two chest radiologists (with 10 and 20 years of experience) independently evaluated 3D spiral UTE VIBE MR image qualities for intrapulmonary vessels, bronchial depiction, artifact/noise, and overall image quality using a five-point scoring system. The scoring system used for intrapulmonary vessels and bronchial depiction was: 1, indistinguishable lobar level; 2, visible lobar vessels/bronchi; 3, visible segmental vessels/bronchi; 4, visible subsegmental vessels/bronchi; and 5, visible sub-subsegmental vessels/bronchi, and the scoring system used for artifact/noise and overall image quality was: 1, unacceptable; 2, poor; 3, fair; 4, good; and 5, excellent.

The two readers reviewed chest CT images by consensus to evaluate pulmonary nodules, other lung abnormalities, and significant lymph nodes (LNs) and independently reviewed 3D spiral UTE VIBE MR images two weeks after CT reviews to prevent recall influencing 3D spiral UTE VIBE MR assessments. The sizes, compositions, and lobar locations of pulmonary nodules were evaluated on chest CT and MR images. Nodule size was defined as mean nodule diameter as determined by the two readers, and lobar location as one of the following five lobes: right upper, right middle, right lower, left upper, or left lower. Using chest CT as the reference standard, the detection rate of pulmonary nodules using the UTE sequence was calculated. LNs with a short axis diameter of >1 cm or cortical thickening were considered significant. The short axis diameter and location (axilla, internal mammary, supraclavicular, and mediastinal area) of significant LNs were assessed on chest CT and MR images. Disagreements between the two readers were resolved by consensus.

Statistical analysis

Inter-observer agreements for the semi-quantitative analysis of image quality on spiral 3D UTE MRI were analyzed using the kappa statistic. The detection rates of pulmonary nodules and lung abnormalities on spiral 3D UTE MR images were evaluated using chest CT images as the reference standard, and diagnostic accuracy of the UTE

Table 1 Characteristics of 93 enrolled patients with breast cancer

Characteristics	Values
Age, years, median [range]	52.5 [32–80]
Cancer type, n	
Ductal carcinoma *in situ*	9
Invasive cancer	84
Invasive ductal carcinoma	72
Invasive lobular carcinoma	4
Other	8
Interval between CT and MRI, days, median [range]	5.2 [0–28]

CT, computed tomography; MRI, magnetic resonance imaging.

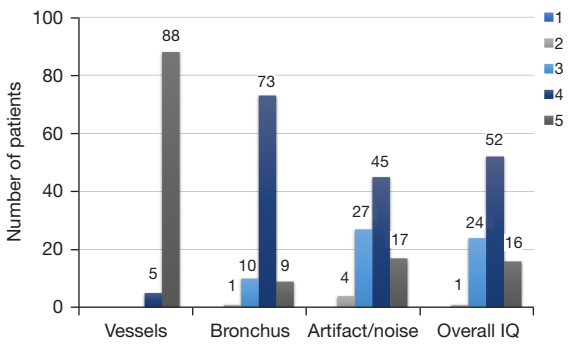

Figure 2 Semi-quantitative analysis of the image quality of spiral 3D UTE MRI for 93 patients with breast cancer. The scoring systems used for intrapulmonary vessels and bronchial depiction were as follows: 1, indistinguishable lobar level; 2, visible lobar vessels/bronchi; 3, visible segmental vessels/bronchi; 4, visible subsegmental vessels/bronchi; and 5, visible sub-subsegmental vessels/bronchi. The scoring systems for artifact/noise and overall image quality were as follows: 1, unacceptable; 2, poor; 3, fair; 4, good; and 5, excellent. IQ, image quality; 3D, three-dimensional; UTE, ultrashort echo time; MRI, magnetic resonance imaging.

sequence for predicting LN metastasis was determined using pathologic diagnosis as the reference standard. The analyses were performed using SPSS version 26.0 (IBM Corp., Armonk, NY, USA), and statistical significance was accepted for P values <0.05.

Results

Patient characteristics

Ninety-three women (mean age, 52.5 years: age range, 32–80 years) were enrolled in the study; baseline characteristics of the enrolled patients are detailed in *Table 1*. Mean time between CT and MRI was 5.2 days (range, 0–28 days).

Semi-quantitative analysis of image quality

Semi-quantitative analysis results of the image quality of spiral 3D UTE VIBE MRI for the 93 patients are presented in *Figure 2*. Intrapulmonary vessels were visible up to the sub-subsegmental [94.6% (88/93)] or subsegmental [5.4% (5/93)] levels on spiral 3D UTE MR images, and bronchial walls up to the sub-subsegmental [9.7% (9/93)], subsegmental [78.5% (73/93)], or segmental [10.8% (10/93)] levels. Images of 95.7% (89/93) and 98.9% (92/93) of patients were better than fair with respect to artifact/noise and overall image quality.

Semi-quantitative analysis of spiral 3D UTE MR image quality showed all inter-observer agreements were statistically significant (P<0.05) and were excellent for intrapulmonary vessels (k=0.795) and good for bronchial depiction, artifact/noise, and overall image quality (k=0.601, 0.624, and 0.649, respectively).

Characteristics and detection rates of pulmonary nodules

Pulmonary nodule measurements obtained by spiral 3D UTE VIBE MRI and chest CT are summarized in *Table 2*. Ninety-four pulmonary nodules were identified by chest CT; 13 ground glass opacity nodules (GGNs) (mean, 4.5 mm; range, 1.2–7.3 mm) and 81 solid nodules (mean, 4.9 mm; range, 1.6–13.7 mm). Of the 81 solid nodules, 14 were calcified, and 67 were non-calcified.

The overall nodule detection rate of spiral 3D UTE MRI was 62.8% (59/94) (*Table 2*, *Figure 3*). No GGN detected by CT was identified by spiral 3D UTE MRI (*Figure 4*). Fifty-nine (72.8%) of the 81 solid nodules detected by CT were detected by spiral 3D UTE MRI. All five solid nodules ≥10 mm in diameter were identified by spiral 3D UTE MRI (100.0%). Of 28 solid nodules with a diameter of 5–10 mm, 26 (92.9%) nodules were detected by spiral 3D UTE MRI. The detection rate for solid nodules of <5 mm in diameter was 58.3% (28/48). Five (35.7%) of the 14 calcified nodules were not detected by spiral 3D UTE VIBE MRI; all 5 had a diameter of <3 mm.

Seventeen (85.0%) of 20 other lung abnormalities detected by CT were detected by spiral 3D UTE MRI. Bronchiectasis [100.0% (2/2)], bronchiolitis [100.0% (2/2)], radiation fibrosis [100.0% (1/1)], subsegmental atelectasis

Table 2 Characteristics and detection rate of pulmonary nodules

Parameters	Spiral 3D UTE	CT (reference)	Detection rate (%)
No. of overall nodules detected	59	94	62.8
No. of GGNs	0	13	0
Mean diameter, mm	0.0 (0.0–0.0)	4.5 (1.2–7.3)	
No. of solid nodules	59	81	72.8
Mean diameter, mm	5.0 (1.8–14.2)	4.9 (1.6–13.7)	
Nodule composition			
Calcified	9	14	64.3
Non-calcified	50	67	74.6
Nodule size			
<5 mm	28	48	58.3
≥5 and <10 mm	26	28	92.9
≥10 mm	5	5	100
Nodule location			
Right upper lobe	12 (5, calcified)	19 (7, calcified)	63.2
Right middle lobe	8 (0, calcified)	11 (1, calcified)	72.7
Right lower lobe	14 (3, calcified)	20 (4, calcified)	70.0
Left upper lobe	13 (1, calcified)	15 (1, calcified)	86.7
Left lower lobe	12 (0, calcified)	16 (1, calcified)	75.0

Data are presented as numbers or mean (range). 3D, three-dimensional; UTE, ultrashort echo time; CT, computed tomography; GGN, ground glass opacity nodule.

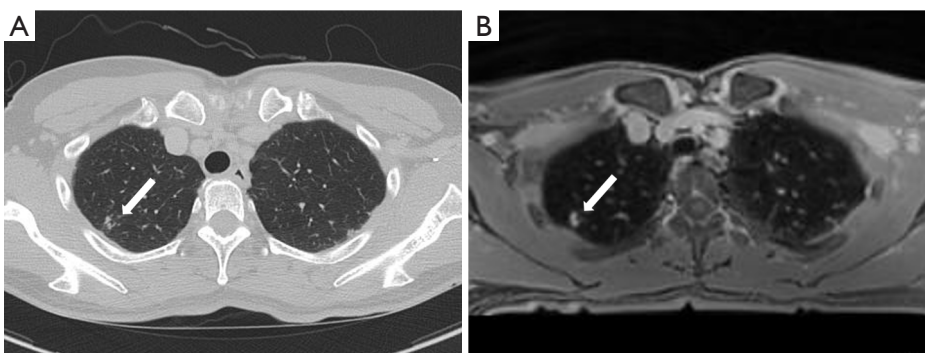

Figure 3 A 61-year-old woman with invasive ductal carcinoma of the right breast. (A) Lung window image of axial non-enhanced CT scan at the level of upper trachea showing two clustered small nodules (arrow) in the right upper lobe. (B) Contrast-enhanced axial T1-weighted 3D spiral UTE VIBE with fat saturation image at the same level showing two clustered small nodules (arrow) in the right upper lobe. CT, computed tomography; 3D, three-dimensional; UTE, ultrashort echo time; VIBE, volume interpolated breath-hold examination.

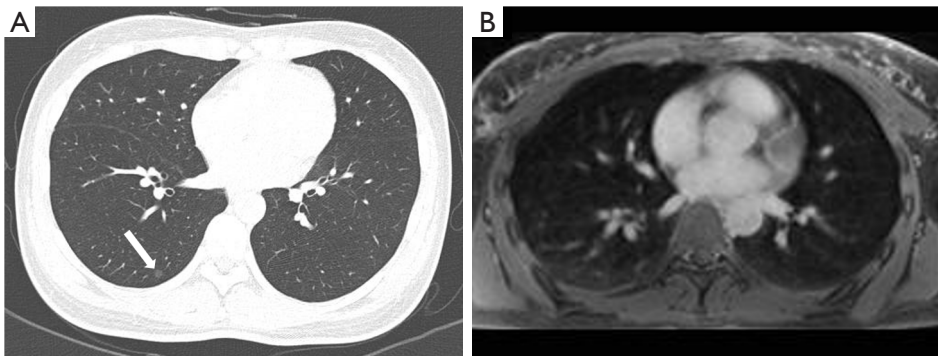

Figure 4 A 46-year-old woman with invasive ductal carcinoma of the right breast. (A) Lung window image of axial non-enhanced CT scan at the right inferior pulmonary vein level showing a 5 mm-sized ground glass opacity nodule (arrow) in the right lower lobe superior segment. (B) Contrast-enhanced axial T1-weighted 3D spiral UTE VIBE with fat saturation image at the same level showing no nodule in the right lower lobe. CT, computed tomography; 3D, three-dimensional; UTE, ultrashort echo time; VIBE, volume interpolated breath-hold examination.

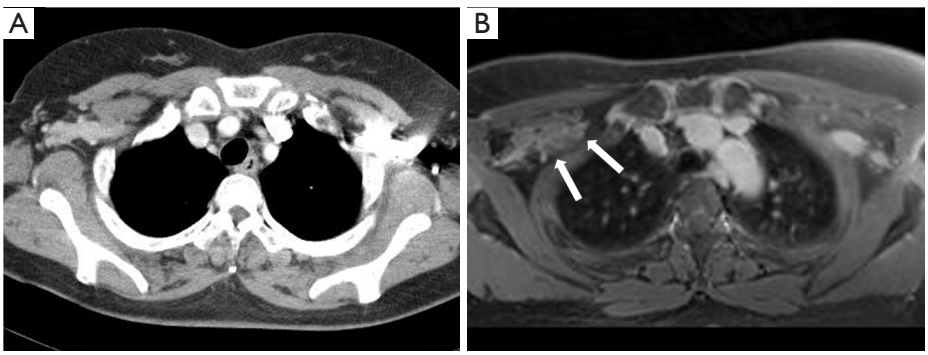

Figure 5 A 54-year-old woman with biopsy-proven invasive ductal carcinoma of the right breast. (A) Contrast-enhanced axial CT image showing no enlarged lymph node at right axilla level II. (B) Contrast-enhanced axial T1-weighted 3D spiral UTE VIBE with fat saturation image showing multiple enlarged lymph nodes with eccentric cortical thickening (two arrows) at right axilla level II, which were confirmed metastatic by pathologic examination. CT, computed tomography; 3D, three-dimensional; UTE, ultrashort echo time; VIBE, volume interpolated breath-hold examination.

or atelectasis [100.0% (6/6)], subinvoluted thymus [100.0% (1/1)], anterior mediastinal nodule [100.0% (1/1)], non-specific interstitial pneumonia [100.0% (1/1)] were all detected on spiral 3D UTE MRI. However, old pulmonary tuberculosis [60.0% (3/5)] and pulmonary emphysema [0.0% (0/1)] were not detected by 3D UTE MRI.

Assessment of LN metastasis

Chest CT detected 69 LNs of mean diameter of 9.0±4.0 mm (range, 3.0–22.0 mm), while spiral 3D UTE MRI detected 70 LNs of mean diameter 9.3±4.5 mm (range, 3.0–21.0 mm) (*Figure 5*). Of the 69 LNs detected by chest CT, 67 were located in the axillary area, one in the internal mammary area, and one in the supraclavicular area. Similarly, of the LNs detected by spiral 3D UTE MRI, 68 were located in the axillary area, one in the internal mammary area, and one in the supraclavicular area.

Of the 79 patients with pathologic diagnoses of an axillary LN, 24 patients had axillary LN metastasis. The sensitivity, specificity, positive predictive value, and negative predictive value for axillary LN metastasis of CT and spiral 3D UTE MRI were 41.7% (10/24), 90.9% (50/55), 66.7% (10/15), 78.1% (50/64) and 41.7% (10/24), 89.1% (49/55), 62.5% (10/16), and 77.8% (49/63), respectively. Thus, the diagnostic accuracy of spiral 3D UTE MRI for predicting axillary LN metastasis was similar to that of chest CT.

Discussion

The lung is one of the most common metastatic sites in breast cancer patients. In particular, 60–70% of metastatic breast cancer patients who eventually died are diagnosed with lung metastasis (20). Thus, breast cancer patients should undergo repeated chest CTs to check for pulmonary metastasis. We investigated the feasibility of chest spiral 3D UTE VIBE MRI in breast cancer patients with respect to the detection of intrathoracic metastasis. Our results are summarized as follows: (I) intrapulmonary vessels and bronchial walls were visible up to the sub-subsegmental and sub-subsegmental levels, respectively, on spiral 3D UTE MR images; (II) 95.7% and 98.9% of patients had spiral 3D UTE MR images of better than fair quality for artifact/noise and overall image quality; (III) the detection rate of spiral 3D UTE MRI for all CT detected pulmonary nodules was 62.8% (59/94) and for solid nodules ≥5 mm in diameter was 93.9% (31/33); (IV) Significant LNs in the axillary area were similarly detected by spiral 3D UTE MRI and chest CT.

As regards image quality, intrapulmonary vessels and bronchial walls were consistently visible on spiral 3D UTE images to the sub-subsegmental level [94.6% (88/93)] and subsegmental level [88.2% (82/93)]. Regarding artifact/noise and overall image quality, spiral 3D UTE MR image qualities were better than fair [95.7% (89/93)] and 98.9% (92/93), respectively. These results concur with those of Cha *et al.* (1), who also found spiral 3D UTE MRI consistently visualized intrapulmonary vessels and bronchial walls at the sub-subsegmental [96.9% (31/32)] and subsegmental [90.6% (29/32)] levels. Additionally, 93.8% (30/32) and 93.8% (30/32) of patients had images of above fair quality for artifact/noise and overall image quality. Furthermore, analysis of images obtained using a breath-hold T1-weighted gradient-echo sequence showed the visibility of intrapulmonary vessels was 80.0% (8/10) at the sub-subsegmental level, and no case showed visibility of the bronchial wall at up to the subsegmental level (21). These results indicate that the spiral 3D UTE sequence can provide high-quality images of the lungs in semi-quantitative analysis, which is considered highly beneficial for lung evaluations.

The overall detection rate for pulmonary nodules by spiral 3D UTE MRI was 62.8%, and of these, 72.8% were solid nodules; no GGNs were found. Cha *et al.* reported an overall nodule detection rate for spiral 3D UTE MRI of 86%, which was superior to our result of 62.8%. However, we attribute this difference to the exclusion of CT-detected lung calcifications and fissural nodules from their analysis (1). In our study, the detection rate of spiral 3D UTE MRI for solid nodules of ≥5 mm was 93.9%, and that of solid nodules of <5 mm was 58.3%. For solid nodules, previous studies have reported detection rates of 60% to 90% for 5 to 8 mm diameter lesions and detection rates close to 100% for ≥8 mm lesions (22-24). Burris *et al.* reported a pulmonary nodule detection rate of 17% for nodules >2 mm but <4 mm in diameter and 83% for nodules ≥4 mm in diameter (83%) (11). Our results largely mirror these findings. Different respiratory states during imaging acquisition may explain the lower detection rates of MRI as chest CT is typically performed at end inspiration and MRI at end expiration, which could result in inadequate lung expansion during MRI and suboptimal detection of small lung nodules. Fortunately, most nodules of <10 mm present a low malignancy risk and are of particularly low risk when located <10 mm from pleura (25). In the present study, of 14 calcified nodules, 5 (35.7%) were not detected by 3D spiral UTE VIBE MRI, and all were <3 mm in diameter. Thoracic calcifications have various signals on T1- and T2-weighted images, as signal intensities depend on their compositions of aggregates of calcium salts and particle sizes (26). Because calcium salts do not contain mobile protons, they have no signal on MRI, and thus, densely calcified lesions are sometimes reported as having low signal intensity on T1- and T2-weighted images, which means they are difficult to detect by lung MRI (26). However, considering that most calcified nodules are benign, our findings indicate that spiral 3D UTE sequences would be more useful for evaluating pulmonary metastasis in clinical practice.

Significant LNs in the axillary area were similarly detected by chest CT and spiral 3D UTE MRI, but were identified in one case more on spiral 3D UTE sequence. The LNs found in the spiral 3D UTE sequence but not in the chest CT were located at axillary level II and were not detected because their densities were the same as that of surrounding pectoralis muscles by chest CT (*Figure 5*). Significant LNs in the internal mammary area and supraclavicular area were similarly detected by chest CT and spiral 3D UTE MRI. Furthermore, the diagnostic accuracies of the modalities for detecting axillary LN metastasis were similar.

This study has several limitations. First, it is limited by its single-center, retrospective design, although data were collected prospectively. Second, correlations between

imaging findings and pathologic nodule results were not possible. Instead, chest CT was performed at <30 days after MRI, and CT results were used as reference standards. However, the differentiation of benign and malignant nodules by even chest CT remains challenging. Third, we included patients with newly diagnosed breast cancer who underwent preoperative breast MRI, and thus pulmonary metastasis was only observed in one patient.

Conclusions

In conclusion, we found that chest spiral 3D UTE VIBE MRI detected pulmonary nodules in breast cancer patients with a 62.8% overall nodule detection rate, a 72.8% solid nodule detection rate, and a 93.9% solid nodule (≥5 mm) detection rate, which was clinically significant and produced images of acceptable quality. Therefore, this study shows that preoperative breast MRI, including a chest spiral 3D UTE sequence, could be used to evaluate breast cancer, axillary LNs, and intrathoracic metastasis simultaneously without radiation exposure, potentially offering a viable alternative to chest CT in patients with breast cancer. However, the low detection rate of chest spiral 3D UTE MRI for GGNs and its limited detection of calcified nodules require improvement.

Acknowledgments

Funding: This work was supported by a 2-Year Research Grant from Pusan National University.

Footnote

Reporting Checklist: The authors have completed the STROBE reporting checklist. Available at https://jtd.amegroups.com/article/view/10.21037/jtd-23-1006/rc

Data Sharing Statement: Available at https://jtd.amegroups.com/article/view/10.21037/jtd-23-1006/dss

Peer Review File: Available at https://jtd.amegroups.com/article/view/10.21037/jtd-23-1006/prf

Conflicts of Interest: All authors have completed the ICMJE uniform disclosure form (available at https://jtd.amegroups.com/article/view/10.21037/jtd-23-1006/coif). YJJ repots a 2-Year Research Grant from Pusan National University. The other authors have no conflicts of interest to declare.

Ethical Statement: The authors are accountable for all aspects of the work in ensuring that questions related to the accuracy or integrity of any part of the work are appropriately investigated and resolved. The study was conducted in accordance with the Declaration of Helsinki (as revised in 2013). The study protocol was approved by the institutional review board of Pusan National University Hospital (IRB No. 2306-001-127), and informed consent was obtained from all individual participants.

References

1. Cha MJ, Park HJ, Paek MY, et al. Free-breathing ultrashort echo time lung magnetic resonance imaging using stack-of-spirals acquisition: A feasibility study in oncology patients. Magn Reson Imaging 2018;51:137-43.
2. Mayo JR, MacKay A, Müller NL. MR imaging of the lungs: value of short TE spin echo pulse sequences. AJR Am J Roentgenol 1992;159:951-6.
3. Ohno Y, Nishio M, Koyama H, et al. Pulmonary 3 T MRI with ultrashort TEs: influence of ultrashort echo time interval on pulmonary functional and clinical stage assessments of smokers. J Magn Reson Imaging 2014;39:988-97.
4. Dournes G, Grodzki D, Macey J, et al. Quiet Submillimeter MR Imaging of the Lung Is Feasible with a PETRA Sequence at 1.5 T. Radiology 2015;276:258-65.
5. Ohno Y, Koyama H, Yoshikawa T, et al. Pulmonary high-resolution ultrashort TE MR imaging: Comparison with thin-section standard- and low-dose computed tomography for the assessment of pulmonary parenchyma diseases. J Magn Reson Imaging 2016;43:512-32.
6. Gai ND, Malayeri A, Agarwal H, et al. Evaluation of optimized breath-hold and free-breathing 3D ultrashort echo time contrast agent-free MRI of the human lung. J Magn Reson Imaging 2016;43:1230-8.
7. Bannas P, Bell LC, Johnson KM, et al. Pulmonary Embolism Detection with Three-dimensional Ultrashort

Echo Time MR Imaging: Experimental Study in Canines. Radiology 2016;278:413-21.
8. Ohno Y, Koyama H, Yoshikawa T, et al. Standard-, Reduced-, and No-Dose Thin-Section Radiologic Examinations: Comparison of Capability for Nodule Detection and Nodule Type Assessment in Patients Suspected of Having Pulmonary Nodules. Radiology 2017;284:562-73.
9. Roach DJ, Crémillieux Y, Serai SD, et al. Morphological and quantitative evaluation of emphysema in chronic obstructive pulmonary disease patients: A comparative study of MRI with CT. J Magn Reson Imaging 2016;44:1656-63.
10. Mahmood K, Ebner L, He M, et al. Novel Magnetic Resonance Imaging for Assessment of Bronchial Stenosis in Lung Transplant Recipients. Am J Transplant 2017;17:1895-904.
11. Burris NS, Johnson KM, Larson PE, et al. Detection of Small Pulmonary Nodules with Ultrashort Echo Time Sequences in Oncology Patients by Using a PET/MR System. Radiology 2016;278:239-46.
12. Ohno Y, Takenaka D, Yoshikawa T, et al. Efficacy of Ultrashort Echo Time Pulmonary MRI for Lung Nodule Detection and Lung-RADS Classification. Radiology 2022;302:697-706.
13. Landini N, Orlandi M, Occhipinti M, et al. Ultrashort Echo-Time Magnetic Resonance Imaging Sequence in the Assessment of Systemic Sclerosis-Interstitial Lung Disease. J Thorac Imaging 2023;38:97-103.
14. Johnson KM, Fain SB, Schiebler ML, et al. Optimized 3D ultrashort echo time pulmonary MRI. Magn Reson Med 2013;70:1241-50.
15. Shin T, Lustig M, Nishimura DG, et al. Rapid single-breath-hold 3D late gadolinium enhancement cardiac MRI using a stack-of-spirals acquisition. J Magn Reson Imaging 2014;40:1496-502.
16. Qian Y, Boada FE. Acquisition-weighted stack of spirals for fast high-resolution three-dimensional ultra-short echo time MR imaging. Magn Reson Med 2008;60:135-45.
17. Mugler Iii JP, Fielden SW, Meyer CH, et al. Breath-hold UTE lung imaging using a stack-of-spirals acquisition. Proceedings of the 23rd Annual Meeting of ISMRM, Toronto, Canada 2015:1476.
18. Dournes G, Yazbek J, Benhassen W, et al. 3D ultrashort echo time MRI of the lung using stack-of-spirals and spherical k-Space coverages: Evaluation in healthy volunteers and parenchymal diseases. J Magn Reson Imaging 2018;48:1489-97.
19. Cha MJ, Ahn HS, Choi H, et al. Accelerated Stack-of-Spirals Free-Breathing Three-Dimensional Ultrashort Echo Time Lung Magnetic Resonance Imaging: A Feasibility Study in Patients With Breast Cancer. Front Oncol 2021;11:746059.
20. Dan Z, Cao H, He X, et al. A pH-Responsive Host-guest Nanosystem Loading Succinobucol Suppresses Lung Metastasis of Breast Cancer. Theranostics 2016;6:435-45.
21. Biederer J, Reuter M, Both M, et al. Analysis of artefacts and detail resolution of lung MRI with breath-hold T1-weighted gradient-echo and T2-weighted fast spin-echo sequences with respiratory triggering. Eur Radiol 2002;12:378-84.
22. Biederer J, Schoene A, Freitag S, et al. Simulated pulmonary nodules implanted in a dedicated porcine chest phantom: sensitivity of MR imaging for detection. Radiology 2003;227:475-83.
23. Cieszanowski A, Lisowska A, Dabrowska M, et al. MR Imaging of Pulmonary Nodules: Detection Rate and Accuracy of Size Estimation in Comparison to Computed Tomography. PLoS One 2016;11:e0156272.
24. Meier-Schroers M, Kukuk G, Homsi R, et al. MRI of the lung using the PROPELLER technique: Artifact reduction, better image quality and improved nodule detection. Eur J Radiol 2016;85:707-13.
25. Hanamiya M, Aoki T, Yamashita Y, et al. Frequency and significance of pulmonary nodules on thin-section CT in patients with extrapulmonary malignant neoplasms. Eur J Radiol 2012;81:152-7.
26. Zampieri JF, Pacini GS, Zanon M, et al. Thoracic calcifications on magnetic resonance imaging: correlations with computed tomography. J Bras Pneumol 2019;45:e20180168.

Cite this article as: Nam KJ, Kang T, Lee JW, Hwang M, Kim JY, Yeom JA, Jeong YJ. Feasibility of chest spiral 3D ultrashort echo time magnetic resonance imaging for intrathoracic metastasis work-up in breast cancer. J Thorac Dis 2023;15(10):5485-5493. doi: 10.21037/jtd-23-1006

